Heliyon 9 (2023) e18789

Contents lists available at ScienceDirect

Heliyon

journal homepage: www.cell.com/heliyon

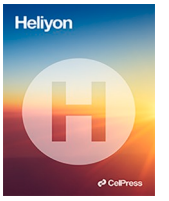

MiR-520d-3p suppresses the proliferation and epithelial-mesenchymal transition of cervical cancer cells by targeting ZFP36L2

Yuan Zhang *, Fei Tian, Jing Zhao

Department of Gynecology, Hebei General Hospital, Shijiazhuang, Hebei, China

ARTICLE INFO

Keywords:
Cervical cancer
miR-520d-3p
ZFP36L2
Proliferation
Epithelial-mesenchymal transition

ABSTRACT

MiR-520d-3p has recently been reported to have anti-tumor function in several cancers, including glioma and gastric cancer. However, the biological function and its mechanism of action remain unclear in cervical cancer (CC). In this study, we observed that miR-520d-3p expression was lowly expressed in CC specimens compared with adjacent normal specimens using reverse transcription quantitative PCR. Moreover, low miR-520d-3p expression was correlated with FIGO stage and lymph node metastasis by Chi-square test. Functionally, overexpression of miR-520d-3p suppressed the proliferation and migration and invasion of two CC cell lines (HeLa and SiHa) using CCK-8 assay and wound healing assay. After target prediction, luciferase reporter assay showed that zinc finger protein 36 ring finger protein-like 2 (ZFP36L2) was a direct target of miR-520d-3p in CC cells. The expression levels of ZFP36L2 at protein and mRNA were significantly increased in CC tissues compared with adjacent tissues. The expression of ZFP36L2 was negatively correlated with miR-520d-3p in the patients with CC. Importantly, ZFP36L2 overexpression abolished the effects of miR-520d-3p on cell proliferation, migration and EMT process in CC cells. In conclusion, our findings indicate that targeting miR-520d-3p/ZFP36L2 axis might be a promising therapeutic target for CC treatment.

1. Introduction

Cervical cancer (CC) is the most frequently diagnosed malignant epithelial tumor in female reproductive tract with 604,127 new cases and 341,831 deaths in 2020 worldwide [1]. Many risk factors, including tobacco, poor immune system, and especially HPV infection, have been reported to be associated with the development of CC [2]. Despite advance in surgery, chemotherapy and radiotherapy/immunotherapy, recurrence and metastasis remain the primary reasons for the failure of these treatment options, particularly in patients at advanced stage (FIGO stage III–IV) with less than 10% five-year survival rate [3–5]. With the development of targeted tumor therapy [6], it is of great significance to explore the molecular mechanism affecting malignant CC cellular behaviors.

Most studies focus on non-coding RNAs (ncRNAs), especially microRNAs (miRNAs) that are a group of highly-conserved small double-stranded endogenous RNAs with 19–24 nucleotides [7]. MiRNAs could negatively regulate gene expression at post-transcriptional level by binding to the 3′-untranslated region (3′-UTR) of their target mRNAs [8]. Identified as essential regulators,

* Corresponding author. Department of Gynecology, Hebei General Hospital, No. 348 Western Peace Road, Xinhua District, Shijiazhuang, 050051, Hebei, China.
E-mail address: 65005865@qq.com (Y. Zhang).

https://doi.org/10.1016/j.heliyon.2023.e18789
Received 3 March 2023; Received in revised form 26 July 2023; Accepted 27 July 2023
Available online 28 July 2023

Abbreviations

CC	cervical cancer
ZFP36L2	Zinc finger protein (ZFP) 36 like 2
3′-UTRs	3′-untranslated regions
EMT	epithelial-mesenchymal transition
CCK-8	Cell Counting Kit-8
OD	optical density
WT	wild-type
MUT	mutant
HRP	horseradish peroxidase

miRNAs play important roles in the progression of multiple cancers, including CC via regulating various biological processes, such as proliferation, apoptosis and metastasis [9–11]. It has been reported that miRNAs serve as oncogenes or tumor suppressors, mainly depending on the modulation of targeted downstream genes or signaling pathways [12]. Among them, miR-520d-3p has been revealed to a key modulator in different types of cancers. For example, overexpression of miR-520d-3p dramatically inhibited the proliferation, cell cycle progression, and migration of gastric cancer cells [13]. Overexpression of miR-520d-3p showed a significant inhibitory effect on cell proliferation and accompanied cell cycle G0/G1 arrest in glioma cells [14]. In addition, miR-520d-3p exerted suppressive effects on cell proliferation and migration in breast cancer [15], hepatocellular carcinoma [16] and melanoma [17]. However, the functional role of miR-520d-3p in CC and its mechanism of action have not been reported yet.

Zinc finger protein (ZFP) 36 like 2 (ZFP36L2, also known as TIS11D, ERF2, and BRF2) is a member of the tristetraprolin (TTP) family members that can interfere with post-transcriptional modifications and protein translation by directly binding to specific AU-rich elements (AREs) located in the 3′-UTR of mRNA molecules [18,19]. Early studies have revealed the tumor suppressive effect of ZFP36L2 in colorectal cancer [20], ovarian [21] and breast cancer [22]. Subsequently, Liu et al. [23] showed that overexpression of ZFP36L2 in leukemia cells could inhibit the cell proliferation and induce the cell apoptosis. Nevertheless, recent studies pointed the oncogenic role of ZFP36L2 as follows: Yonemori et al. [24] confirmed the overexpression of ZFP36L2 in pancreatic ductal adenocarcinoma (PDAC) clinical specimens and demonstrated that silencing ZFP36L2 inhibited cancer cell aggressiveness. Moreover, ZFP36L2 has oncogenic and chemosensitive characteristics in glioblastoma through regulating cell proliferation, cell cycle arrest and apoptosis [25]. These findings indicate that the dysregulation of ZFP36L2 expression plays a key role in cancer development.

In this study, we determined the expression of miR-520d-3p and its correlation with clinical characteristics in CC patients. After confirmed the relationship between miR-520d-3p and ZFP36L2, we further investigated the functional role of miR-520d-3p/ZFP36L2 axis in affecting CC cell proliferation, migration and epithelial-mesenchymal transition (EMT) process, aiming to provide a feasible basis for CC diagnosis and therapy.

Table 1
The association between miR-520d-3p expression and clinicopathological characteristics of cervical cancer patients.

Characteristics	Cases (n = 57)	miR-520d-3p expression		*P*-values
		Low (n = 29)	High (n = 28)	(chi-square test)
Age (year)				0.494
<50	32	15	17	
≥50	25	14	11	
Tumor size (cm)				0.113
<4	42	24	18	
≥4	15	5	10	
FIGO stage				0.039*
I-II	38	23	15	
III	19	6	13	
Differentiation				0.760
Well, moderate	48	24	24	
Poor	9	5	4	
HPV status				0.325
Negative	35	16	19	
Positive	22	13	9	
Lymph node metastasis				0.003*
Negative	39	25	14	
Positive	18	4	14	

Note: *$p < 0.05$; FIGO, international federation of gynecology and obstetrics.

2. Materials and methods

2.1. Clinical specimens

A total of 57 paired tumor tissues and matched adjacent non-cancerous tissues were collected from CC patients underwent surgical resection between January 2019 and December 2020 at Hebei General Hospital (Hebei, China). Any therapeutics were confirmed not to be performed in all patients with signed written informed consent before surgery. All collected tissues were clinically diagnosed by experimented pathologists according to the pathological classification system of the International Federation of Gynecology and Obstetrics (FIGO) [26], and immediately frozen in liquid nitrogen until further analysis. Some important clinical characteristics of the patients were listed in Table 1. This study was performed in accordance with the Declaration of Helsinki and approved by the Medical Research Ethics committee of the Hebei General Hospital (Approval no. HGH-623A, Hebei, China).

2.2. Cell culture and transfection

Two CC cell lines (HeLa and SiHa) and the non-tumorigenic epithelial cell line HaCaT acquired from ATCC were cultured in DMEM supplemented with 10% FBS (Thermo Fisher Scientific, Waltham, MA, USA), 10 mM glutamine, 1% penicillin (100 U/ml)/streptomycin (100 μg/ml) in a humidified incubator containing 5% CO_2 at 37 °C. The miR-520d-3p mimics and its negative control (NC mimics) were purchased from GenePharma Co. Ltd (Shanghai, China). The pcDNA3.1 overexpression vector was used for generating the pcDNA-ZFP36L2 construct and vector alone was utilized as NC. For cell transfection, HeLa and SiHa cells (2×10^5) were inoculated into six-well plates and transfection with miR-520d-3p mimics, NC mimics, constructed plasmids alone or together for 48 h using the Lipofectamine 3000 (Invitrogen, Carlsbad, CA).

2.3. CCK-8 assay

The CC cell proliferation was assessed by performing Cell Counting kit-8 (CCK-8) assay. In brief, CC cells were harvested at 48 h post-transfection and seeded into 96-well plates with 5,000 cells per well. At 24, 48, and 72 h, cells were incubated with 10 μl CCK-8 solution (Beyotime, Shanghai, China) for an additional 2 h at 37 °C. Subsequently, the optical density (OD) of each well was determined at a wavelength of 450 nm using a microplate reader. Each assay was performed in triplicate and repeated three times.

2.4. Wound healing assay

The migration ability of transfected CC cells was analyzed via wound-healing method. Cells were cultured in six-well plates at a density of 5×10^5 cells per well to reach 90% confluency. Afterwards, the scratch was drawn with a 10 μl pipette tip and corresponding scratch width was recorded as 0 h width (W0). Following 24 h-incubation, the wound scratch was photographed and scratch width was recorded as 24 h width (W24) using a phase contrast microscope at 100× magnification (Olympus IX81, Tokyo, Japan). Based on the formula: (W0 – W24)/W0 × 100%, we calculated relative migration distance to assess CC cell migration ability. Each assay was performed in triplicate and repeated three times.

2.5. Dual luciferase reporter assay

The wild-type (WT) and mutated (MUT) ZFP36L2 plasmids based on the predicted binding sites between miR-520d-3p and the 3′-untranslated regions (UTRs) of ZFP36L2 were constructed using the psiCHECK-2 vector (Promega, Madison, USA). Next, HeLa and SiHa cells were co-transfected with miR-520d-3p mimics or NC mimics and either the WT-ZFP36L2 or MUT-ZFP36L2 plasmid using Lipofectamine 3000 for 48 h. Relative luciferase activity in each group was examined in accordance with the instructions of a Dual Luciferase Reporter Assay Kit (Promega).

2.6. Reverse transcription quantitative PCR

Using TRIzol reagent (Takara, Japan), we first extracted total RNA sample from tissues or cell lines and then performed reverse transcription with RevertAid First Strand cDNA Synthesis Kit (Thermo Fisher Scientific). Reverse transcription quantitative PCR was conducted with SYBR Green PCR mix (Takara Biotechnology Co., Ltd., Dalian, China) on 7300 Real-Time PCR System (Applied Biosystems, USA). The primers used in this study were listed as follows: miR-520d-3p, forward: 5′- GGTCTACAAAGGGAAGC-3′ and reverse: 5′-TTTGGCACTAGCACATT-3’; U6, forward: 5′-CTCGCTTCGGCAGCACA-3′ and reverse: 5′-AACGCTTCACGAATTTGCGT-3′ [16]; ZFP36L2, forward: 5′- ATCAACTCCACGCGCTACAA-3′ and reverse: 5′- GGCAGAAGCCGATGGTATGA-3′ (https://www.ncbi.nlm.nih.gov/tools/primer-blast/primertool.cgi?ctg_time=1686543667&job_key=4ug869z50VH2b9Rq2QrwWKMR4WqOAvp3jw); GAPDH, forward: 5′-GGTGAAGGTCGGAGTCAACG-3′ and reverse: 5′-GCATCGCCCCACTTGATTTT-3′ (https://www.ncbi.nlm.nih.gov/tools/primer-blast/primertool.cgi?ctg_time=1686544670&job_key=gYteHInQhHijRp5DkyO6cek4q0PEK7BexQ). Relative expression levels of miR-520d-3p and ZFP36L2 were calculated with $2^{-\Delta\Delta Ct}$ method.

2.7. Western blot analysis

Total protein sample from cell lines was extracted with RIPA lysis buffer (Sigma-Aldrich, USA) and corresponding protein concentration was determined with a BCA protein assay kit (Beyotime). Equal amount of protein sample was separated by 12% SDS-PAGE and transferred onto PVDF membranes (Millipore). After blocked with 5% non-fat milk for 2 h at room temperature, the membranes were incubated with primary antibodies against ZFP36L2, E-cadherin, N-cadherin, Vimentin and GAPDH (Abcam, Cambridge, MA, USA) overnight at 4 °C. Following incubation with corresponding secondary antibodies for 2 h at room temperature, the protein bands were visualized with Chemiluminescence Substrate Kit (Thermo Fisher Scientific).

2.8. Immunohistochemistry

CC and adjacent tissues were fixed in 10% neutral buffered formalin, embedded in paraffin and made into 4-μm thick sections. The sections were deparaffinized in xylene, rehydrated with graded alcohol and underwent antigen repair. Afterwards, the sections were blocked with 3% H_2O_2 for 5 min and incubated with ZFP36L2 primary antibody (PA5-61513, Thermo Fisher Scientific) at 4 °C overnight, followed by incubation with biotinylated anti-goat horseradish peroxidase (HRP)-conjugated secondary antibody (ab150077, Abcam) for 2 h at room temperature. Subsequently, the sections were treated with DAB for 10 min and counterstained with hematoxylin-erosin for 5 min. The immunohistochemical staining of ZFP36L2 in human smooth muscle showed strong cytoplasmic positivity as positive control. Negative control was composed of mixture with no primary antibody but normal goat serum instead. After dehydrated in ethanol, the immunohistochemical staining of each sample was scored depending on staining intensity (0, no staining; 1, weak; 2, moderate; 3, strong staining) and the percentage of stained cells (0–3: 0, 0–5%; 1, 6–20%; 2, 21–60%; 3, 61–100%) under a light microscope at 100 or 200 × magnification. The final staining was classified into weak, moderate and strong staining with the sum of the intensity an extent score 0–1, 2–4 and 5, respectively, as described previously [27,28].

2.9. Statistical analysis

All the statistical analyses were performed with GraphPad Prism 8.0 (GraphPad Software, La Jolla, CA, USA). The expression levels of miR-520d-3p/ZFP36L2 were compared between tumor tissues and adjacent tissues using Wilcoxon signed rank test. Chi-square test was used to analyze the relationship between miR-520d-3p/ZFP36L2 expression and clinical characteristics in CC patients. The normality of the data distribution was statically analyzed by the Shapiro–Wilk test (sample size less than 5000) with a p-value >0.05. Pearson's correlation analysis was performed to evaluate the correlation between the expression of miR-520d-3p and ZFP36L2. Quantitative data were expressed as mean ± SD of three independent experiments. Comparison of difference between two groups was conducted by Students' t-test. Multiple group comparisons were realized by one-way ANOVA followed by Dunnett's test or Tukey's post-hoc test. The p-value of less than 0.05 was accepted as statistically significant difference.

3. Results

3.1. Reduced miR-520d-3p expression was observed in CC and correlated with poor prognostic parameters

Reverse transcription quantitative PCR was first performed to examine the expression levels of miR-520d-3p in the 57 paired normal-cancer cervical tissues. As shown in Fig. 1A, miR-520d-3p expression was significantly lower in CC tissues compared with that in adjacent tissues. Based on the median of miR-520d-3p expression, 57 CC patients were divided into low and high miR-520d-3p expression groups to analyze the relationship between miR-520d-3p expression and clinical characteristics. As summarized in Table 1, decreased miR-520d-3p expression was associated with FIGO stage ($p = 0.039$) and lymph node metastasis ($p = 0.003$). In addition, we found that miR-520d-3p expression was also remarkedly downregulated in two cancerous cell lines (HeLa and SiHa), in

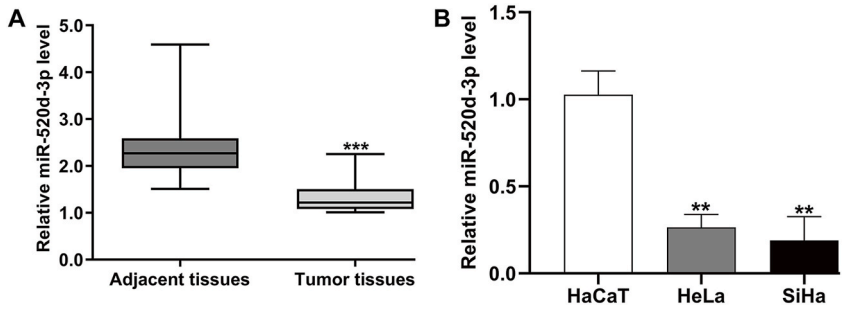

Fig. 1. Reduced miR-520d-3p expression was observed in CC tissues and cells. (A) The expression of miR-520d-3p was assessed by reverse transcription quantitative PCR in CC tissues (n = 57) and adjacent non-tumor tissues (n = 57). ***$p < 0.001$, compared with adjacent tissues; (B) The miR-520d-3p expression level was also confirmed using reverse transcription quantitative PCR in the non-tumorigenic epithelial cell line HaCaT and two CC cell lines (HeLa and SiHa). **$p < 0.01$, compared with HaCaT; The values presented as mean ± SD (n = 3).

comparison with the non-tumorigenic epithelial cell line HaCaT (Fig. 1B).

3.2. Upregulation of miR-520d-3p attenuated the proliferative and migratory abilities of the CC cells

Considering the downregulation of miR-520d-3p in CC, we performed the gain of function assays to explore the biological function of miR-520d-3p *in vitro*. First, miR-520d-3p mimics or NC mimics was transfected into HeLa and SiHa cells to construct miR-520d-3p overexpression cell models. After 48 h transfection, a significant increase in miR-520d-3p expression level was confirmed by reverse transcription quantitative PCR (Fig. 2A). Subsequently, the CCK-8 assay results showed that the cell proliferation of HeLa and SiHa cells was markedly attenuated in the miR-520d-3p mimics group compared to the NC mimic group (Fig. 2B). Next, wound healing assay was conducted to evaluate cell migration ability. As depicted in Fig. 2C, upregulation of miR-520d-3p significantly decreased the relative migration rate from 51.6% ± 2.1% to 24.8% ± 1.3% in HeLa cells and from 56.1% ± 1.9% to 32.7% ± 2.1% in SiHa cells.

3.3. ZFP36L2 was a direct target gene of miR-520d-3p

To explore the potential molecular mechanisms underlying miR-520d-3p affecting CC cells, we used the target prediction website TargetScan and focused on the ZFP36L2 gene already reported in several tumors. The website predicted the 3′-UTR of ZFP36L2 mRNA contains a complementary sequence for the seed region of miR-520d-3p. Based on this, we constructed the wild type and mutant plasmids of miR-520d-3p 3′-UTR (Fig. 3A). The targeted regulatory effects of miR-520d-3p on ZFP36L2 was further verified by luciferase reporter assay. The results showed that miR-520-3p overexpression dramatically decreased the luciferase activity of WT-ZFP36L2 but did not affect that of MUT-ZFP36L in HeLa (Fig. 3B) and SiHa (Fig. 3C) cells. Next, we discovered that the expression levels of ZFP36L2 at mRNA (Fig. 3D) and protein (Fig. 3E) were both significantly downregulated in HeLa and SiHa cells after miR-520-3p mimics transfection, when compared with NC mimics transfection. Collectively, these findings showed that miR-520d-3p negatively regulated ZFP36L2 via targeting its 3′-UTR in CC cells.

3.4. Increased ZFP36L2 expression in CC tissues was negatively correlated with miR-520d-3p

Next, we performed immunohistochemistry staining to determine the expression of ZFP36L2 in CC tissues and adjacent tissues. As shown in Fig. 4A, we observed a significant elevation in the moderate and strong staining of ZFP36L2 protein in CC tissues compared with those in adjacent tissues. Moreover, increased ZFP36L2 protein expression was significantly related with tumor size ($p = 0.019$) and lymph node metastasis ($p = 0.004$) (Table 2). To explore the association between ZFP36L2 and miR-520d-3p in CC, we analyzed the expression of ZFP36L2 mRNA. Consistent with immunohistochemistry results, ZFP36L2 mRNA levels were notably higher in CC tissues than those in adjacent tissues (Fig. 4B). Afterwards, correlation analysis results showed that the expression of ZFP36L2 was

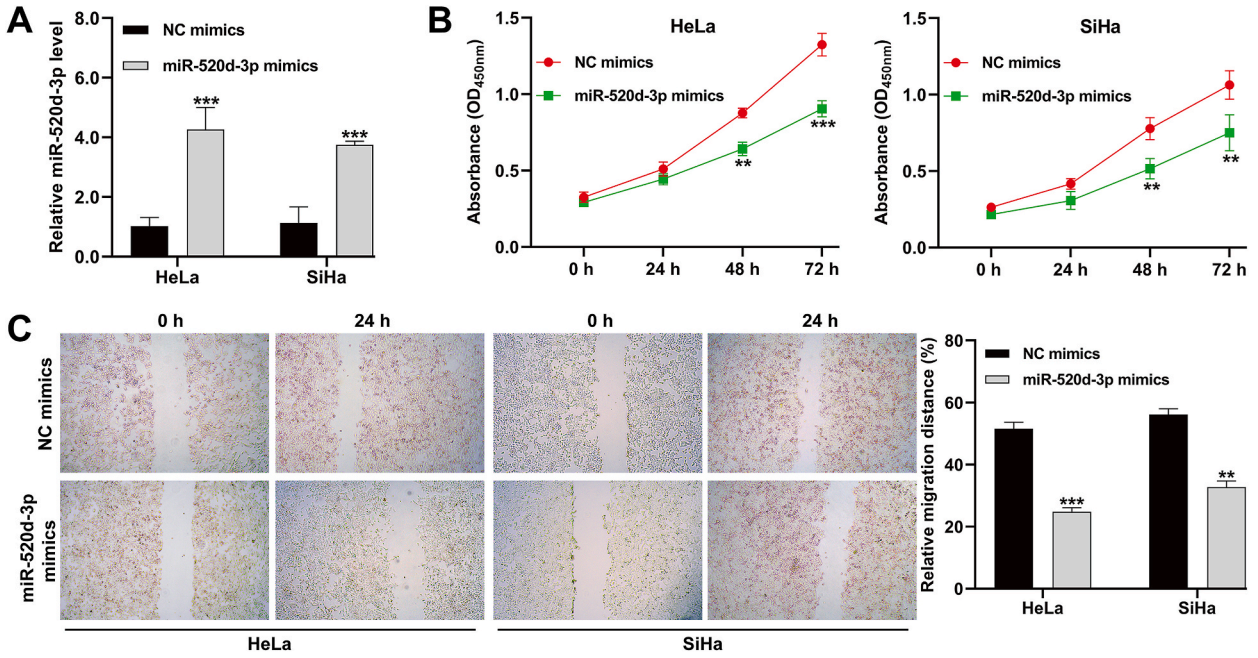

Fig. 2. Upregulation of miR-520d-3p attenuated the proliferative and migratory abilities of the CC cells. The miR-520d-3p mimics or NC mimics was transfected into HeLa and SiHa cells for 48 h. (A) Transfection efficiency was confirmed by reverse transcription quantitative PCR. (B) Cell proliferation was determined by CCK-8 assay in transfected HeLa and SiHa cells. (C) A wound healing assay was utilized to evaluate the migration of transfected HeLa and SiHa cells. The values presented as mean ± SD (n = 3). $^{**}p < 0.01$, $^{***}p < 0.001$, compared with NC mimics.

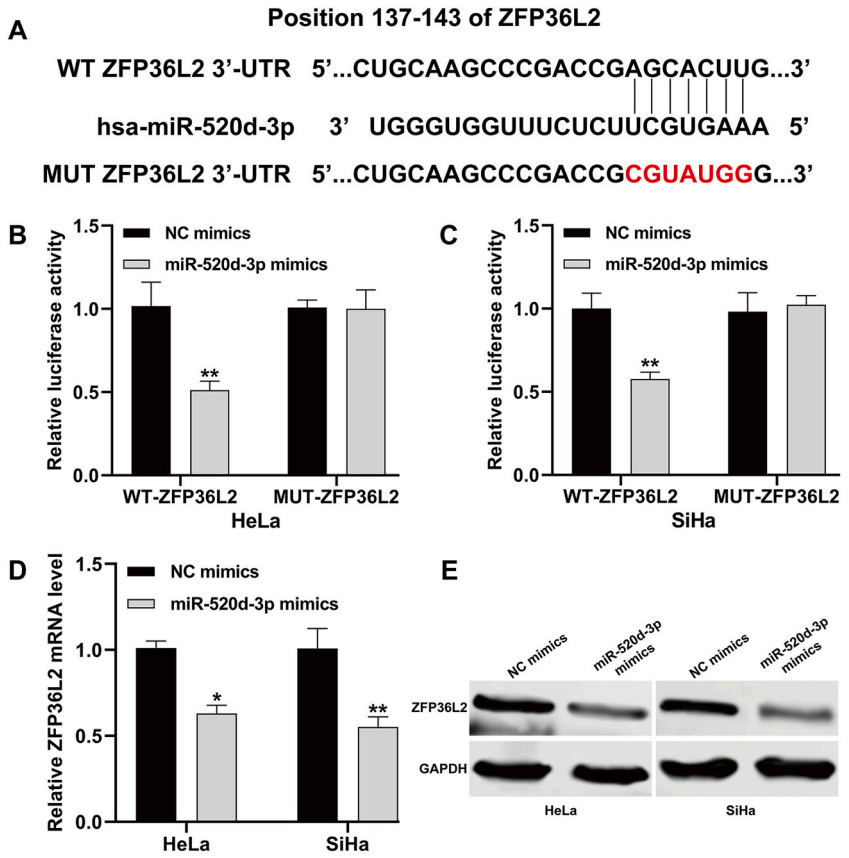

Fig. 3. ZFP36L2 was a direct target gene of miR-520d-3p. (A) Complementarity of the 3′-UTR of wild-type (WT) or mutant (MUT) human ZFP36L2 mRNA with the miR-520d-3p seed sequence. (B, C) Relative luciferase activity in HeLa and SiHa cell line co-transfected with NC mimics/miR-520d-3p mimics and ZFP36L2-WT/MUT plasmid. (D) Reverse transcription quantitative PCR analyses of ZFP36L2 mRNA expression in HeLa and SiHa cells following transfection of miR-520d-3p mimics or NC mimics. The values presented as mean ± SD (n = 3). $*p < 0.05$, $**p < 0.01$, compared with NC mimics. (E) Western blotting results of ZFP36L2 expression following transfection of NC mimics and miR-520d-3p mimics into HeLa and SiHa cells.

negatively correlated with miR-520d-3p in the patients with CC (Fig. 4C).

3.5. *Overexpression of ZFP36L2 rescued the effects of miR-520d-3p on CC cell proliferation and migration*

To further investigate whether ZFP36L12 was the downstream regulator involved in miR-520d-3p regulating CC cell functions, pcDNA-ZFP36L2 and miR-520d-3p mimics were transfected into HeLa and SiHa cells individually or in combination. Western blot analysis not only confirmed the overexpression of ZFP36L2 in HeLa and SiHa cells after pcDNA-ZFP36L2 transfection alone (Fig. 4A), but also demonstrated that decreased ZFP36L12 induced by miR-520d-3p mimics was obviously reversed after co-transfection with pcDNA-ZFP36L2 and miR-520d-3p mimics (Fig. 5B). Subsequently, the results from CCK-8 assay revealed miR-520d-3p overexpression significantly reduced the proliferation of HeLa (Fig. 5C) and SiHa (Fig. 5D) cells, but the reduced cell proliferation due to miR-520d-3p mimics was markedly reversed by pcDNA-ZFP36L2. Additionally, the suppressed cell migratory ability of HeLa and SiHa cells by miR-520d-3p overexpression was greatly reversed after co-transfection with pcDNA-ZFP36L2 and miR-520d-3p mimics (Fig. 5E and F). Furthermore, the impact of miR-520d-3p/ZFP36L2 axis on EMT process was examined via Western blot. As described in Fig. 5G, overexpression of ZFP36L2 obviously rescued the promotive role of miR-520d-3p on E-cadherin expression and the suppressive effects of miR-520d-3p on the expression levels of N-cadherin and Vimentin in HeLa and SiHa cells.

4. Discussion

Even though the diagnosis and treatment for CC have been greatly improved in recent years, the five-year survival rate of CC still remain unsatisfactory, especially those advanced and metastatic patients [29]. Among various therapeutic approaches, gene therapy has caused great interests for researchers. With the deepening of miRNA research, more and more studies have elucidated that investigation of gene expression, biological function and associated mechanisms of cancer-related miRNAs in CC may provide novel therapeutic targets for this disease [30,31]. In the present study, we first observed that miR-520d-3p expression was significantly

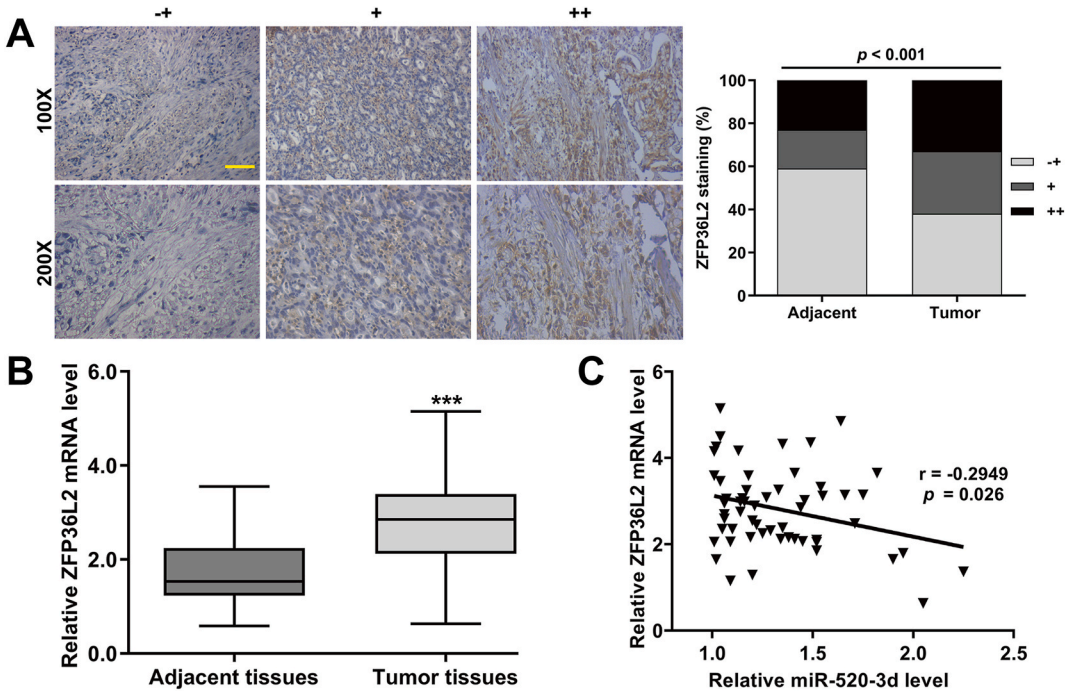

Fig. 4. Increased ZFP36L2 expression in CC tissues was negatively correlated with miR-520d-3p. (A) Representative images of different degrees of ZFP36L2 immunohistochemistry staining (-+, weak staining, + moderate staining, ++ strong staining) (left panel) and the percentage of ZFP36L2 high in CC tissues was significantly higher than that in adjacent normal tissues (right panel). Scale bar = 100 μm. (B) The expression of ZFP36L2 mRNA was detected by reverse transcription quantitative PCR in the 57 patients with CC. The values presented as mean ± SD (n = 3). ***$p < 0.001$, compared with adjacent tissues; (C) The correlation between the expression of ZFP36L2 and miR-520d-3p was analyzed by Pearson's correlation analysis.

Table 2
Relationship between ZFP36L2 expression and clinicopathological characteristics of cervical cancer patients.

Characteristics	Cases (n = 57)	ZFP36L2 expression		*P*-values
		Positive (n = 35)	Negative (n = 22)	(chi-square test)
Age (year)				0.366
<50	32	18	14	
≥50	25	17	8	
Tumor size (cm)				0.019*
<4	42	22	20	
≥4	15	13	2	
FIGO stage				0.124
I-II	38	26	12	
III	19	9	10	
Differentiation				0.724
Well, moderate	48	29	19	
Poor	9	6	3	
HPV status				0.405
Negative	35	20	15	
Positive	22	15	7	
Lymph node metastasis				0.004*
Negative	39	19	20	
Positive	18	16	2	

Note: *$p < 0.05$; FIGO, international federation of gynecology and obstetrics.

down-regulated in CC tissues and cells lines. Moreover, lower miR-520d-3p expression was associated with FIGO stage and lymph node metastasis in CC patients. Similarly, Li et al. [13] showed that lower expression of miR-520d-3p was associated with tumor invasion, lymph nodes metastasis, a higher clinical stage and poorer overall survival in gastric cancer. Xiang et al. [16] presented the decreased expression of miR-520d-3p was associated with large tumor diameter, venous infiltration, and advanced TNM stage in hepatocellular carcinoma. Furthermore, miR-520d-3p has been reported to be downregulated and correlated with worse prognosis in ovarian cancer [32], astrocytomas [33], and hemangioma [34]. These evidences indicate that miR-520d-3p could also be a potential tumor suppressor

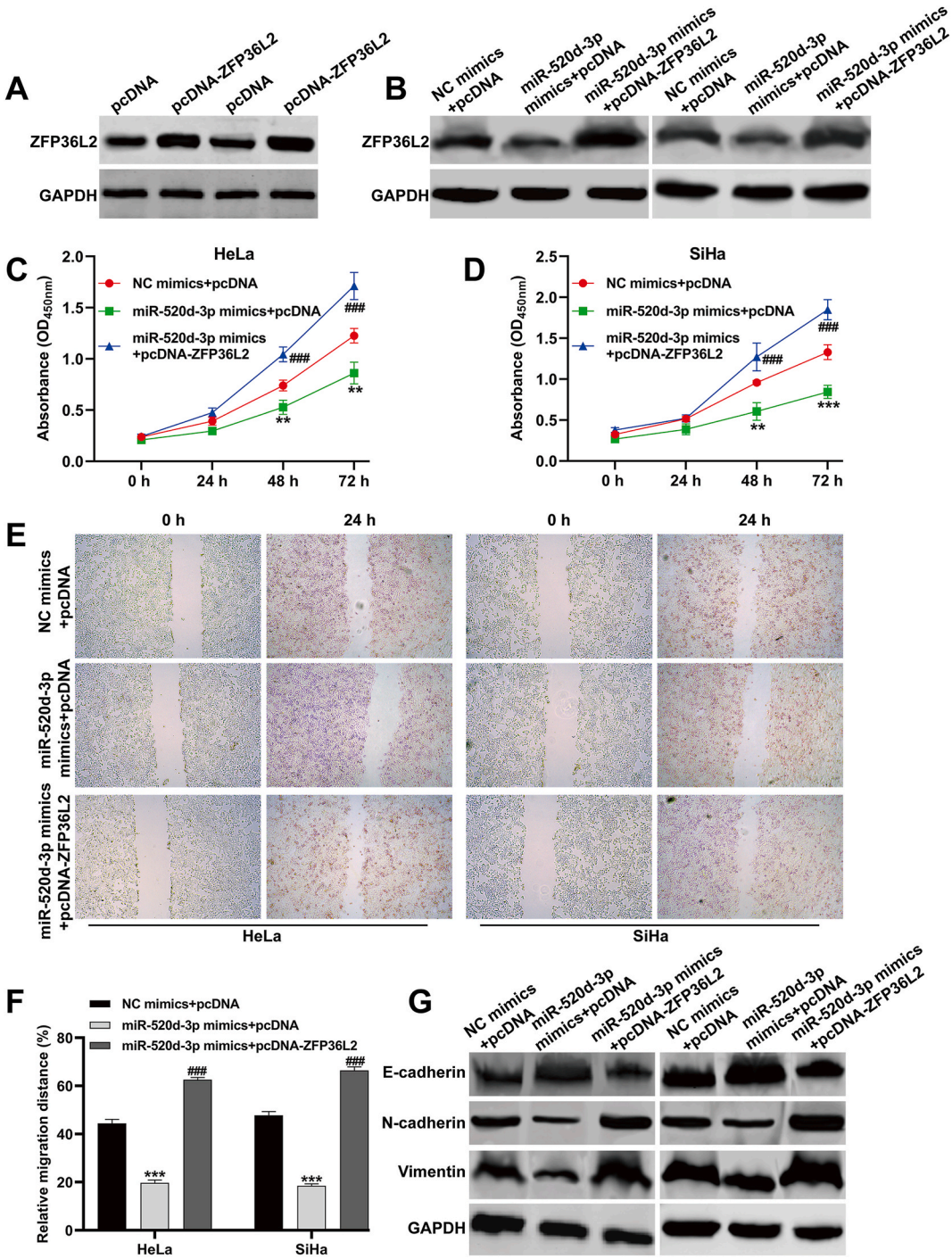

Fig. 5. Overexpression of ZFP36L2 rescued the effects of miR-520d-3p on CC cell proliferation and migration. HeLa and SiHa cells were transfected with pcDNA-ZFP36L2 and the miR-520d-3p mimics individually or in combination. (A) The overexpression of ZFP36L2 was confirmed by Western blot analysis in HeLa and SiHa cells transfected with pcDNA-ZFP36L2 individually. (B) ZFP36L2 overexpression reversed the suppressive effect of miR-520d-3p mimics on ZFP36L2 expression. (C, D) Cell proliferation was determined by CCK-8 assay in transfected HeLa and SiHa cells. (E, F) A wound healing assay was utilized to evaluate the migration of transfected HeLa and SiHa cells. The values presented as mean ± SD (n = 3). $^{**}p < 0.01$, $^{***}p < 0.001$, compared with NC mimics + pcDNA; $\#\#\#p < 0.001$, compared with miR-520d-3p mimics + pcDNA; (G) The protein levels of E-cadherin, N-cadherin and Vimentin were detected by Western blot analysis in transfected HeLa and SiHa cells.

of CC.

Data from *in vitro* assays indicated that overexpression of miR-520d-3p inhibited proliferation and migration of HeLa and SiHa cells. In agreement with our data, restoration of miR-520d-3p expression reduced cell viability by causing the accumulation of cell apoptosis in breast cancer [15] and melanoma [17]. Upregulation of miR-520d-3p dramatically inhibited the cell proliferation, migration and invasion of gastric cancer [13] and hepatocellular carcinoma [16]. Most recently, Yao et al. [35] also manifested that miR-520d-3p overexpression suppressed the proliferation, migration, invasion, and promotes the adhesion of osteosarcoma cells. As our best knowledge, miRNAs regulate biological features of tumor cells by binding to the 3'-UTR of the target gene. It has been reported that miR-520d-3p directly targets certain oncogenes to exert its suppressive effects in tumor cells, which include pituitary tumor transforming gene 1 (PTTG1) in glioma [14], anti-silencing function 1B histone chaperone (ASF1B) in melanoma [17], spindle and kinetochore associated 2 (SKA2) in breast cancer [15] and MIG-7 in osteosarcoma [35]. In this work, the target gene of miR-520d-3p was identified and ZFP36L2 was selected as the candidate target. Further study indicated that ZFP36L2 expression level was negatively regulated by miR-520d-3p in CC cells.

ZFP36L2 is zinc finger protein 36, C3H type-like 2 (also known as Brf2, Erf2 and Tis11D), which has been previously reported to have important functions in several types of cancers [36]. In colorectal cancer cell lines, forced expression of ZFP36L2 inhibited cell proliferation and cyclin D gene expression [37]. ZFP36L2 has been identified as a novel AML1 target gene, could suppress cell proliferation, induced cell-cycle arrest and apoptosis of leukemia cells [23]. Deletion of ZFP36L2 leads to perturbed thymic development and T lymphoblastic leukemia, indicating its antitumor functions [38]. In contrast to these studies, we showed that a significant increase in ZFP36L2 expression was found in CC clinical specimens. Importantly, re-expression of ZFP36L2 overcame the inhibitory effects of miR-520d-3p on CC cells. Consistent with our data, ZFP36L2 protein expression was upregulated in glioblastoma and ZFP36L2 inhibition led to decreased cell proliferation in temozolomide-resistant LN18 cells [25]. Overexpression of ZFP36L2 was confirmed in PDAC clinical specimens and involved in tumor-suppressive miR-375-mediated PDAD molecular network [24]. We further assessed the character of miR-520d-3p/ZFP36L2 axis on the cellular EMT process through the detection of EMT-related molecules. It is well known that EMT, a key transition stage from epithelial cells to mesenchymal cells [39], is closely related with changes of cancer invading abilities [40]. Loss of epithelial markers, such as E-cadherin and α-catenin, and acquisition of mesenchymal markers, such as N-cadherin, and vimentin are the hallmarks of the EMT process [41]. Consistent with the decreased CC cell migration induced by miR-520d-3p/ZFP36L2 axis, our data showed that overexpression of ZFP36L2 reversed the upregulation of E-cadherin and downregulation of N-cadherin and vimentin induced by miR-520d-3p mimics in HeLa and SiHa cells. All these evidences confirmed that miR-520d-3p are available for depletion of the proliferation and EMT of CC cells by downregulating ZFP36L2.

In summary, the present study described that decreased miR-520-3p expression was associated with poor prognostic parameters. Overexpression of miR-520d-3p suppressed CC cell proliferation, migration and EMT process. We further revealed the mechanism of the miR-520d-3p-ZFP36L2 axis in CC. Our current findings may provide a valuable theoretical basis for early screening and diagnosis of CC.

Ethics approval and consent to participate

This study was performed in accordance with the Declaration of Helsinki and approved by the Medical Research Ethics committee of the Hebei General Hospital (Approval no. HGH-623A, 2018.8.23; Hebei, China). All individuals signed written informed consent for the use of human specimens for clinical experiments.

Author contribution statement

Yuan Zhang: Conceived and designed the experiments; Performed the experiments; Analyzed and interpreted the data; Wrote the manuscript. Fei Tian: Performed the experiments. Jing Zhao: Contributed reagents, materials, analysis tools or data; Wrote the manuscript.

Data availability statement

Data included in article/supp. material/referenced in article.

Declaration of competing interest

The authors declare that they have no known competing financial interests or personal relationships that could have appeared to influence the work reported in this paper.

Appendix A. Supplementary data

Supplementary data to this article can be found online at https://doi.org/10.1016/j.heliyon.2023.e18789.

References

[1] H. Sung, J. Ferlay, R.L. Siegel, M. Laversanne, I. Soerjomataram, A. Jemal, F. Bray, Global cancer statistics 2020: GLOBOCAN estimates of incidence and mortality worldwide for 36 cancers in 185 countries, CA A Cancer J. Clin. 71 (2021) 209–249.
[2] P. Olusola, H.N. Banerjee, J.V. Philley, S. Dasgupta, Human papilloma virus-associated cervical cancer and health disparities, Cells 8 (2019) 622.
[3] A. Duenas-Gonzalez, S. Campbell, Global strategies for the treatment of early-stage and advanced cervical cancer, Curr. Opin. Obstet. Gynecol. 28 (2016) 11–17.
[4] R.N. Eskander, K.S. Tewari, Immunotherapy: an evolving paradigm in the treatment of advanced cervical cancer, Clin. Therapeut. 37 (2015) 20–38.
[5] P.T. Ramirez, M. Frumovitz, R. Pareja, A. Lopez, M. Vieira, R. Ribeiro, A. Buda, X. Yan, Y. Shuzhong, N. Chetty, et al., Minimally invasive versus abdominal radical hysterectomy for cervical cancer, N. Engl. J. Med. 379 (2018) 1895–1904.
[6] Y.T. Lee, Y.J. Tan, C.E. Oon, Molecular targeted therapy: treating cancer with specificity, Eur. J. Pharmacol. 834 (2018) 188–196.
[7] K. Felekkis, E. Touvana, C. Stefanou, Deltas, C. microRNAs: a newly described class of encoded molecules that play a role in health and disease, Hippokratia 14 (2010) 236–240.
[8] M.A. Valencia-Sanchez, J. Liu, G.J. Hannon, R. Parker, Control of translation and mRNA degradation by miRNAs and siRNAs, Genes Dev. 20 (2006) 515–524.
[9] M. Li, Y. Xiao, M. Liu, Q. Ning, Z. Xiang, X. Zheng, S. Tang, Z. Mo, MiR-26a-5p regulates proliferation, apoptosis, migration and invasion via inhibiting hydroxysteroid dehydrogenase like-2 in cervical cancer cell, BMC Cancer 22 (2022) 876.
[10] Y. Wang, A. Chen, C. Zheng, L. Zhao, miR-92a promotes cervical cancer cell proliferation, invasion, and migration by directly targeting PIK3R1, J. Clin. Lab. Anal. 35 (2021), e23893.
[11] R. Xiao, H. Wang, B. Yang, MicroRNA-98-5p modulates cervical cancer progression via controlling PI3K/AKT pathway, Bioengineered 12 (2021) 10596–10607.
[12] K. Saliminejad, H.R. Khorram Khorshid, S. Soleymani Fard, S.H. Ghaffari, An overview of microRNAs: biology, functions, therapeutics, and analysis methods, J. Cell. Physiol. 234 (2019) 5451–5465.
[13] R. Li, W. Yuan, W. Mei, K. Yang, Z. Chen, MicroRNA 520d-3p inhibits gastric cancer cell proliferation, migration, and invasion by downregulating EphA2 expression, Mol. Cell. Biochem. 396 (2014) 295–305.
[14] T. Zhi, K. Jiang, X. Xu, T. Yu, W. Wu, E. Nie, X. Zhou, X. Jin, J. Zhang, Y. Wang, et al., MicroRNA-520d-5p inhibits human glioma cell proliferation and induces cell cycle arrest by directly targeting PTTG1, Am. J. Tourism Res. 9 (2017) 4872–4887.
[15] Z. Ren, T. Yang, J. Ding, W. Liu, X. Meng, P. Zhang, K. Liu, P. Wang, MiR-520d-3p antitumor activity in human breast cancer via post-transcriptional regulation of spindle and kinetochore associated 2 expression, Am. J. Tourism Res. 10 (2018) 1097–1108.
[16] Y. Xiang, Y. Huang, H. Sun, Y. Pan, M. Wu, J. Zhang, Deregulation of miR-520d-3p promotes hepatocellular carcinoma development via lncRNA MIAT regulation and EPHA2 signaling activation, Biomed. Pharmacother. 109 (2019) 1630–1639.
[17] X. Shi, X. Xu, N. Shi, Y. Chen, M. Fu, MicroRNA-520d-3p suppresses melanoma cells proliferation by inhibiting the anti-silencing function 1B histone chaperone, Bioengineered 12 (2021) 10703–10715.
[18] S.A. Brooks, P.J. Blackshear, Tristetraprolin (TTP): interactions with mRNA and proteins, and current thoughts on mechanisms of action, Biochim. Biophys. Acta 1829 (2013) 666–679.
[19] C. Molle, T. Zhang, L. Ysebrant de Lendonck, C. Gueydan, M. Andrianne, F. Sherer, G. Van Simaeys, P.J. Blackshear, O. Leo, S. Goriely, Tristetraprolin regulation of interleukin 23 mRNA stability prevents a spontaneous inflammatory disease, J. Exp. Med. 210 (2013) 1675–1684.
[20] F.M. Suk, Y.T. Chen, Y.C. Liang, Abstract 3475: inhibitory effects of ZFP36L1 and ZFP36L2 on the cell proliferation in human colorectal cancer cells, Cancer Res. 77 (2017), 3475-3475.
[21] D.M. Carrick, P.J. Blackshear, Comparative expression of tristetraprolin (TTP) family member transcripts in normal human tissues and cancer cell lines, Arch. Biochem. Biophys. 462 (2007) 278–285.
[22] H.L. Chou, C.T. Yao, S.L. Su, C.Y. Lee, K.Y. Hu, H.J. Terng, Y.W. Shih, Y.T. Chang, Y.F. Lu, C.W. Chang, et al., Gene expression profiling of breast cancer survivability by pooled cDNA microarray analysis using logistic regression, artificial neural networks and decision trees, BMC Bioinf. 14 (2013) 100.
[23] J. Liu, W. Lu, S. Liu, Y. Wang, S. Li, Y. Xu, H. Xing, K. Tang, Z. Tian, Q. Rao, et al., ZFP36L2, a novel AML1 target gene, induces AML cells apoptosis and inhibits cell proliferation, Leuk. Res. 68 (2018) 15–21.
[24] K. Yonemori, N. Seki, H. Kurahara, Y. Osako, T. Idichi, T. Arai, K. Koshizuka, Y. Kita, K. Maemura, S. Natsugoe, ZFP36L2 promotes cancer cell aggressiveness and is regulated by antitumor microRNA-375 in pancreatic ductal adenocarcinoma, Cancer Sci. 108 (2017) 124–135.
[25] M.F. Che Mat, E.A. Mohamad Hanif, N.A. Abdul Murad, K. Ibrahim, R. Harun, R. Jamal, Silencing of ZFP36L2 increases sensitivity to temozolomide through G2/M cell cycle arrest and BAX mediated apoptosis in GBM cells, Mol. Biol. Rep. 48 (2021) 1493–1503.
[26] M. Arbyn, X. Castellsague, S. de Sanjose, L. Bruni, M. Saraiya, F. Bray, J. Ferlay, Worldwide burden of cervical cancer in 2008, Ann. Oncol. : Off. J. Eur. Soci. Med. Oncol. 22 (2011) 2675–2686.
[27] J. Wang, S. Yu, L. Cui, W. Wang, J. Li, K. Wang, X. Lao, Role of SMC1A overexpression as a predictor of poor prognosis in late stage colorectal cancer, BMC Cancer 15 (2015) 90.
[28] J. Ruan, H. Zheng, X. Rong, X. Rong, J. Zhang, W. Fang, P. Zhao, R. Luo, Over-expression of cathepsin B in hepatocellular carcinomas predicts poor prognosis of HCC patients, Mol. Cancer 15 (2016) 17.
[29] W. Wang, L. Li, M. Wu, S. Ma, X. Tan, S. Zhong, Laparoscopic vs. Abdominal radical hysterectomy for locally advanced cervical cancer, Front. Oncol. 9 (2019) 1331.
[30] A. Pedroza-Torres, J. Fernandez-Retana, O. Peralta-Zaragoza, N. Jacobo-Herrera, D. Cantu de Leon, J.F. Cerna-Cortes, C. Lopez-Camarillo, C. Perez-Plasencia, A microRNA expression signature for clinical response in locally advanced cervical cancer, Gynecol. Oncol. 142 (2016) 557–565.
[31] F. Wang, B. Li, X. Xie, The roles and clinical significance of microRNAs in cervical cancer, Histol. Histopathol. 31 (2016) 131–139.
[32] M. Nishimura, E.J. Jung, M.Y. Shah, C. Lu, R. Spizzo, M. Shimizu, H.D. Han, C. Ivan, S. Rossi, X. Zhang, et al., Therapeutic synergy between microRNA and siRNA in ovarian cancer treatment, Cancer Discov. 3 (2013) 1302–1315.
[33] R.P. Deshpande, Y. Chandra Sekhar, M. Panigrahi, P.P. Babu, SIRP alpha protein downregulates in human astrocytoma: presumptive involvement of hsa-miR-520d-5p and hsa-miR-520d-3p, Mol. Neurobiol. 54 (2017) 8162–8169.
[34] W. Zhao, H. Fu, S. Zhang, S. Sun, Y. Liu, LncRNA SNHG16 drives proliferation, migration, and invasion of hemangioma endothelial cell through modulation of miR-520d-3p/STAT3 axis, Cancer Med. 7 (2018) 3311–3320.
[35] N. Yao, J. Zhou, J. Song, Y. Jiang, J. Zhang, miR-520d-3p/MIG-7 axis regulates vasculogenic mimicry formation and metastasis in osteosarcoma, Neoplasma 69 (2022) 764–775.
[36] S. Sanduja, F.F. Blanco, D.A. Dixon, The roles of TTP and BRF proteins in regulated mRNA decay, Wiley Interdis. Rev. RNA. 2 (2011) 42–57.
[37] F.M. Suk, C.C. Chang, R.J. Lin, S.Y. Lin, S.C. Liu, C.F. Jau, Y.C. Liang, ZFP36L1 and ZFP36L2 inhibit cell proliferation in a cyclin D-dependent and p53-independent manner, Sci. Rep. 8 (2018) 2742.
[38] D.J. Hodson, M.L. Janas, A. Galloway, S.E. Bell, S. Andrews, C.M. Li, R. Pannell, C.W. Siebel, H.R. MacDonald, K. De Keersmaecker, et al., Deletion of the RNA-binding proteins ZFP36L1 and ZFP36L2 leads to perturbed thymic development and T lymphoblastic leukemia, Nat. Immunol. 11 (2010) 717–724.
[39] K. Gasior, N.J. Wagner, J. Cores, R. Caspar, A. Wilson, S. Bhattacharya, M.L. Hauck, The role of cellular contact and TGF-beta signaling in the activation of the epithelial mesenchymal transition (EMT), Cell Adhes. Migrat. 13 (2019) 63–75.
[40] R. Qureshi, H. Arora, M.A. Rizvi, EMT in cervical cancer: its role in tumour progression and response to therapy, Cancer Lett. 356 (2015) 321–331.
[41] O. Solheim, M. Forsund, C.G. Trope, S.M. Kraggerud, J.M. Nesland, B. Davidson, Epithelial-mesenchymal transition markers in malignant ovarian germ cell tumors, APMIS : APMIS (Acta Pathol. Microbiol. Immunol. Scand.) 125 (2017) 781–786.